Energy & Environmental Science

Cite this: *Energy Environ. Sci.*, 2011, **4**, 4938

www.rsc.org/ees

COMMUNICATION

The predicted crystal structure of $Li_4C_6O_6$, an organic cathode material for Li-ion batteries, from first-principles multi-level computational methods†

Dong-Hwa Seo,‡[a] Hyungjun Kim,‡[b] Haegyeom Kim,[a] William A. Goddard, III*[bc] and Kisuk Kang*[a]

Received 18th August 2011, Accepted 26th September 2011
DOI: 10.1039/c1ee02410h

In this communication, we use first-principles based multi-level computational methods to predict the crystal structure of $Li_4C_6O_6$, the key intermediate material that can be oxidized to $Li_2C_6O_6$ or reduced to $Li_6C_6O_6$. This predicted structure leads to an X-ray diffraction (XRD) pattern in good agreement with experiment, validating the predicted structure. With this structure in hand one can proceed to determine details for the electrochemical properties of these organic electrodes (chemical potential for Li ion as a function of loading and the mechanism for the lithiation/delithiation process) useful in designing optimum systems.

To achieve the sustainability required for next generation energy storage systems, it is desirable to develop Li rechargeable batteries that involve renewable processes operating at low temperatures with a low CO_2 footprint.[1] This led to the proposal that the inorganic electrodes be replaced with abundant organic materials.[1–3] Among these systems, lithiated oxocarbon salt ($Li_{2+x}C_6O_6$) is considered to be a most promising cathode material due to its high theoretical capacity, 580 mAh g^{-1}, for $x = 0$ to $x = 4$, four times the capacity of the conventional cathode material, $LiCoO_2$.[2] Fundamental to investigating and optimizing the redox reactions of this organic electrode, is the crystal structure of $Li_{2+x}C_6O_6$. Thus X-ray diffraction (XRD) patterns have been reported by Chen *et al.* for $Li_2C_6O_6$ (2008)[2] and $Li_4C_6O_6$ (2009),[3] however, no one yet has been able to solve for the atomic positions within the unit cells of these crystals.

Due to the low electron density of Li, the XRD pattern is dominated by the packing of the C_6O_6 moieties with modest contributions from the Li atoms. However, intercalation of Li into the C_6O_6 framework leads to charge transfer complexes that dramatically affect the energy and packing of the C_6O_6 moieties. Here we combine quantum mechanics (density functional theory, DFT), force-fields (FF) derived from the DFT, and Grand Canonical Monte Carlo (GCMC) to predict the energetics and changes in packing using the following iterative multi-paradigm computational strategy, summarized in Fig. 1:

1. We postulated a variety of hypothetical C_6O_6 frameworks with various packings of the C_6O_6 molecules within a large periodic supercell (containing 8 C_6O_6 units) and used our FF to optimize the geometry (eliminating bad contacts between C_6O_6 molecules).

2. Keeping each C_6O_6 moiety fixed, we carried out GCMC simulations using our FF, to locate the optimum positions of Li ions intercalated within each C_6O_6 framework.

3. We then optimized each of the structures from step 2, using DFT to fully relax the $Li_4C_6O_6$ structure.

4. The above procedure was iterated several times with various starting points to determine the global minimum crystal structure of $Li_4C_6O_6$.

[a]*Department of Materials Science and Engineering, Seoul National University, Seoul, 151-742, Republic of Korea. E-mail: matlgen1@snu.ac.kr; Fax: +82 2 880 8197; Tel: +82 2 880 7088*
[b]*Graduate School of EEWS (WCU), KAIST, Daejeon, 305-701, Republic of Korea*
[c]*Materials and Process Simulation Center, California Institute of Technology, 1200 East California Boulevard, Pasadena, CA, 91125, USA. E-mail: wag@wag.caltech.edu; Fax: +626 585 0918; Tel: +626 395 2731*

† Electronic supplementary information (ESI) available: Energies, crystal structure parameters and XRD patterns of stable structures and experimental details. See DOI: 10.1039/c1ee02410h

‡ These authors contributed equally to this project.

Broader context

In recent years, there have been growing demands on organic electrode materials for sustainable Li rechargeable batteries. $Li_{2+x}C_6O_6$ were suggested as promising organic cathode materials due to a high theoretical capacity and the abundance of raw materials. However, the unknown crystal structure of $Li_{2+x}C_6O_6$ is a major hurdle to investigating and optimizing this cathode material. This communication provides the crystal structure of $Li_4C_6O_6$ predicted with a new multi-level strategy. We show that $Li_4C_6O_6$ has three different Li sites, two inter-layer sites and one intra-layer site, as well as determining their chemical potentials for lithium extraction. Our findings provide insights about the nature of intermolecular interactions, redox reactions, lithium diffusion, *etc.*, which are useful in designing improved organic cathode materials. This multi-level computational method may also be helpful in predicting the crystal structure of other metal-intercalated molecular crystal structures.

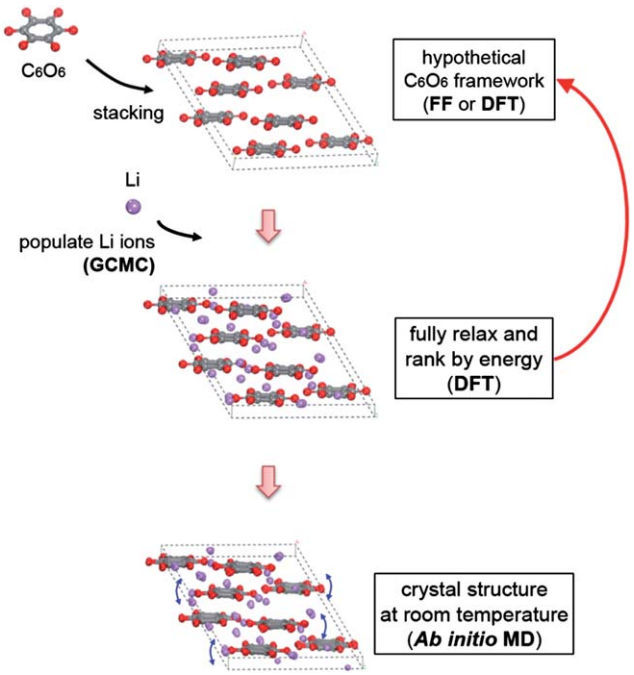

Fig. 1 Schematic of our multi-level computational method.

The list of $Li_4C_6O_6$ structures from step 4 was ranked according to the DFT energies and their predicted XRD patterns were compared with the experimental XRD. Starting with this best structure, we carried out molecular dynamics (MD) simulation at 300 K using forces from the DFT (termed *ab initio* MD or Car–Parrinello MD) to take into account fluctuations due to temperature. Finally the averaged XRD pattern from the 300 K dynamics is compared with experiment.

We applied the above procedure, starting from two distinct hypothetical C_6O_6 framework structures;

1) The ($2a \times 2b \times c$) crystal structure of $H_4C_6O_6 \cdot 2H_2O$ (the precursor for synthesis of $Li_4C_6O_6$)[3] by removing H and H_2O. The structure of $Li_4C_6O_6$ starting from this is denoted as structure A.

2) The ($a \times b \times c$) crystal structure of $Na_2C_6O_6$[4] by removing Na. The structure of $Li_4C_6O_6$ starting from this is denoted as structure B.

Then, we used GCMC (with our FF) to predict the best locations of Li ions within each C_6O_6 framework, followed by full DFT relaxation of geometry within the simulation cell. The computed XRD patterns of structures A and B are in Figures S1a and S1b.† We see that structure A leads to 2θ values of the major peaks in the XRD pattern that are too far from the experimental peaks, so we ruled out structure A. Indeed, the energy of structure A is significantly higher than that of our predicted global minimum structure by 1.14 eV per formula unit.

In contrast, structure B leads to the main peak at $2\theta = 31.62°$, in close agreement with the 31.6° from experiment. This main peak at 31.6° corresponds to the (004) planes of the proposed structure B, which are parallel to C_6O_6 layers. This suggesting that $Li_4C_6O_6$ has layers of C_6O_6 planes, with a calculated interlayer spacing between C_6O_6 layers (d_{layer}) of 2.83 Å. However, the experimental XRD pattern exhibits a second main peak at $2\theta = 13.7°$ (corresponding to d = 6.46 Å), whereas the computed peak is at 15.46°. At this point, we suspected that the d = 6.46 Å spacing is related to stacking sequences of different layers and we sheared each layer with respect to the next by changing the β cell parameter by 30° while retaining the interlayer spacing since $2d_{layer}/\cos 30° = 6.54$ Å. We then used DFT to fully relax the structure, leading to $\beta \sim 60°$. The new monoclinic structure reproduces the experimental peaks located at 13.7° and 23.9°, while retaining the main peak at 31.6° as shown in Figure S1c.† However, this led to additional peaks resulting from the ordering introduced by the small unit cell (8 C_6O_6) required for the DFT.

To find the most stable stacking pattern, we systematically generated a series of stacking patterns of the C_6O_6 layers by gradually sliding the layers within the delithiated simulation cell. Then we re-introduced the Li atoms using GCMC simulations with our FF. The structure and the cell parameters were fully relaxed again using DFT. The resulting energies and crystal structure parameters of fifty most stable structures among over 300 tested structures are tabulated in Table S2.†

The most stable structure, denoted as C, is shown in Fig. 2. It has the *C*2/*m* space group with lattice parameters of $a = 12.917$ Å, $b = 7.541$ Å, $c = 6.523$ Å, $\alpha = 90°$, $\beta = 119.6°$, and $\gamma = 90°$ (see Table S3 for detailed atomic coordinates†). The computed XRD pattern of the final structure is shown in Fig. 3a. Major peaks at 31.9° and 14.1° show excellent correspondence to the experimental XRD pattern with similar relative intensities. The low intensity peaks at higher angles also match reasonably well with experiments. The slight mismatches remaining between the smaller peaks of the XRD pattern

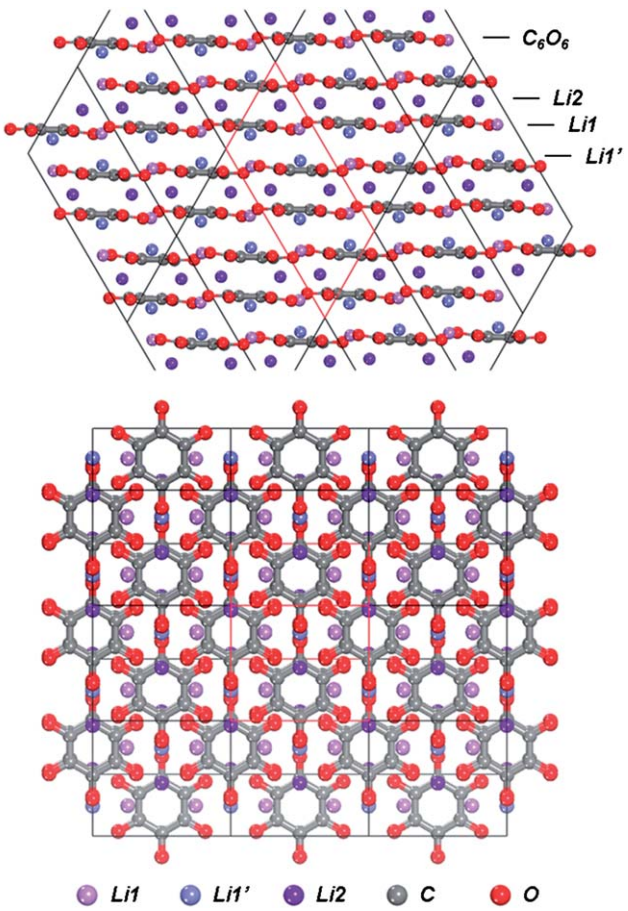

Fig. 2 The predicted global minimum structure of $Li_4C_6O_6$. (Structure C) Various Li sites are presented with different colors. Red monoclinic box indicates unit cell of $Li_4C_6O_6$.

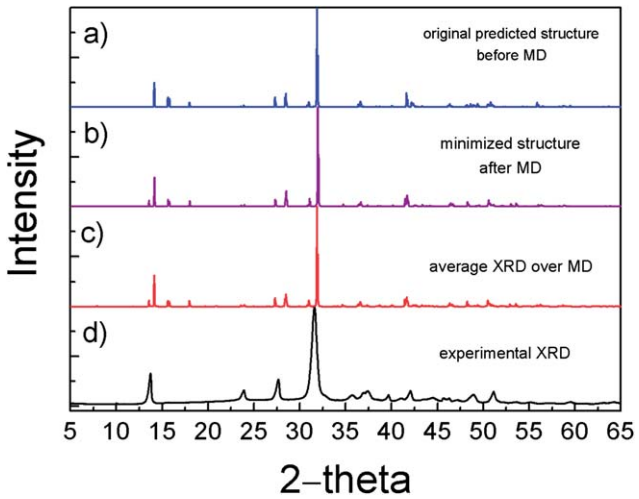

Fig. 3 Comparison of XRD patterns of the final global minimum predicted structure, denoted as structure C, of $Li_4C_6O_6$ with experiment. a) Original predicted structure, b) the minimized structure after 30 ps of *ab initio* MD simulation and c) the averaged XRD pattern over 300 different configurations selected from the MD simulation.

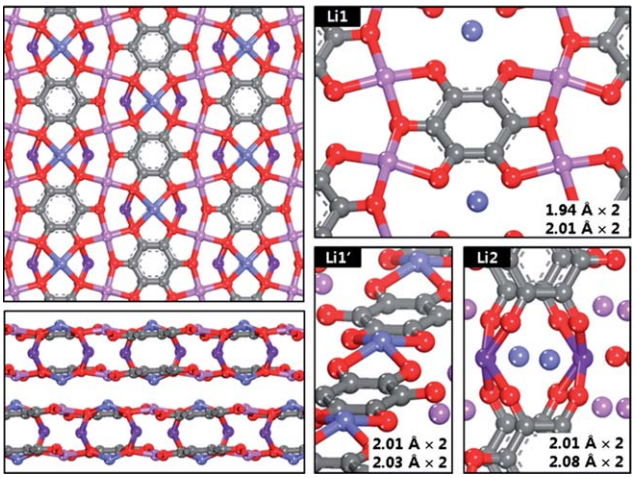

Fig. 4 The three different Li sites of the predicted global minimum structure (C) of $Li_4C_6O_6$. Li–O bond lengths of each Li site are shown.

are probably due to disorder in the structure such as stacking faults, thermal fluctuations (*vide infra*), and thermal expansion in the experimental sample. Nevertheless, the peak at 27.3° is observed as two split peaks from our simulated XRD pattern as compared to a single peak in the experiment. In order to address this discrepancy, we generated over 300 different stacking patterns of C_6O_6 frameworks not far from the structure C. From various stacking sequences of the C_6O_6 layers that we investigated in Table S2,† we found that these stacking faults can alter the peak intensities as well as the peak positions near about 27.3° (Figure S4†). We further found that the energy cost required for the stacking faults is small, *e.g.*, with only up to ~300 meV of energy needed to generate 50 different types of stacking faults within four-layer unit cell system. The presence of stacking faults is relatively common in layered materials.[5,6] In particular, the low temperature synthesis of layered materials often yields to the stacking faults in the structure.[7] Considering the low temperature synthesis (673 K, see supporting information for experimental details†) of the sample, it is expected that structural imperfection such as stacking faults can be easily induced in the experimental sample. The broad nature of experimental XRD peaks is another indirect indication that structural disorder does exist in the experimental sample to some extent. Moreover, we note that the high symmetry imposed in our DFT simulation cell can be broken in the large supercell of the experimental sample due to the defects or thermal fluctuations. We expect that this also can result in mismatches at smaller peaks in the XRD pattern.

We find that every Li atom in the structure is coordinated to four oxygen atoms, which differs from $Na_2C_6O_6$ and $K_2C_6O_6$ where Na and K are coordinated with 8 oxygen ions. This is plausible, resulting from the smaller size of Li. Indeed the Li is known to coordinate to four oxygen ions for the $LiMn_2O_4$ and Li_2NiO_2 cathode materials.[8,9]

We find three types of energetically favorable Li sites in the final $Li_4C_6O_6$ structure: (see Fig. 2 and 4)

1) Li1 site: coordinated by four oxygen ions of two adjacent C_6O_6 molecules in *same* layer,

2) Li2 site: coordinated by four oxygen ions of four C_6O_6 molecules in *neighboring layers*, and

3) Li1′ site: similar to Li1, but slightly shifted from the C_6O_6 layers due to electrostatic repulsion of nearby Li ions at Li1′ site and Li2 site.

The calculated Li–O distances in $Li_4C_6O_6$ range from 1.94 to 2.08 Å (see Fig. 4), which are similar to those in typical Li containing cathodes such as $LiCoO_2$ (2.09 Å) and $LiFePO_4$ (2.09 ~ 2.19 Å).[10,11] The C–C bond lengths range from 1.434 and 1.437 Å, and the C–O bond lengths range from 1.303 and 1.310 Å in our final structure. Such small deviations in bond distances arise because every Li ion coordinates four oxygen atoms within a similar distance, and transfer almost equal charge to each oxygen atom. Therefore, all carbon atoms in the C_6O_6 molecules should have a similar chemical shift, leading to the single peak observed in ^{13}C MAS NMR spectra reported by H. Chen *et al.*[3] We note that these NMR observations show that the crystal cannot consist of isolated $Li_4C_6O_6$ molecules, which has 4 C–C bond lengths of 1.303 Å and 2 of 1.409 Å, which two distinct C–O bond lengths of 1.408 and 1.510 Å (see Figure S5†).

To estimate the chemical potential at each Li position, we used DFT to determine the energy cost to extract one Li atom from the 64 Li atoms of the ($1a \times 2b \times 2c$) supercell of $Li_4C_6O_6$ crystal, but keeping the remaining atoms fixed. This "vertical" or snap chemical potential will be too high, but it is useful for determining which Li is easiest to extract. The chemical potentials of Li1, Li2, and Li1′ are estimated as −5.38, −5.43 and −5.55 eV, respectively. When we include the relaxation of the systems after the lithium extraction, the chemical potentials of Li1, Li2, and Li1′ are estimated as −4.86, −4.99 and −5.07 eV, respectively. This suggests that during the initial delithiation process, Li ions may be extracted mostly from Li1 sites (in-plane sites). Such Li1 vacancies may promote Li diffusion across the layers. Such pathways are not present in $LiCoO_2$ systems because there is no channel across the closed packed cobalt oxide layers.

We then performed *ab initio* MD at 300 K to validate the thermal stability of our predicted structure and to understand how thermal motions would affect the XRD pattern observed at 300 K. After 30 ps of MD simulation we minimized the structure, and found that the structure remains identical to the original one (*cf.* Fig. 3a and 3b). This confirms the stability of our predicted structure. The averaged

diffraction pattern over 300 different configurations from the MD, collected every 100 steps (Fig. 3c) leads to thermally averaged peak intensities that match much more closely to the experimental XRD peaks.

No crystal structure of $Li_2C_6O_6$, $Li_4C_6O_6$, or $Li_6C_6O_6$ have previously been reported; however speculations have considered the $Li_{2+x}C_6O_6$ to have each Li coordinated within a single molecule of $Li_{2+x}C_6O_6$.[12] This is in stark contrast to our predictions in which each Li is coordinated to four oxygen ions of two or four neighboring C_6O_6 units.

We further investigated other possible C_6O_6 packing arrangements to confirm that our procedure has provided a global minimum structure. We used the *Polymorph* module of Materials Studio[13] to randomly generate C_6O_6 frameworks in 14 space groups ($P\bar{1}$, $P2_1$, $C2$, Cc, P_2/m, $P2_1/m$, $C2/m$, $P2/c$, $P2_1/c$, $C2/c$, $P2_12_12_1$, $Pna2_1$, $Pbcn$ and $Pbca$). To efficiently examine the large search domain, we used a Monte Carlo simulated annealing process (MC-SA), and then fully minimized the resulting structures using our FF. These structures were clustered by crystal similarity measure to generate 113 possible C_6O_6 frameworks. Then, we performed our multi-level computational method with these 113 C_6O_6 frameworks to populate Li ions and obtain accurate quantum mechanical energetics. The final DFT energies, crystal structure parameters and XRD patterns of the 20 lower energy structures are tabulated in the ESI (table S7 and figure S8). We find that the original predicted structure is 0.1 to 3.8 eV per formula unit more stable than these 113 additional random stacking structures and that our original structure is in far better agreement with the experimental XRD.

The multi-level computational method used here was validated by showing that the XRD pattern generated from the structure with the lowest DFT energy is in good agreement with the experimental pattern. This allows us to determine the character of the lithium binding sites. We find both inter-layer and intra-layer Li positions suggesting insights into the mechanisms by which this cathode is charged and discharged. This should be useful for considering how to optimize the performance of organic cathode materials for Li rechargeable battery applications. This multi-level strategy may also be helpful in predicting the crystal structure of other metal-intercalated molecular crystal structures.

Computational details

We used the Perdew–Burke–Ernzerhof (PBE) exchange–correlation parameterization (spin-polarized Generalized Gradient Approximation) of DFT[14] as implemented in the Vienna *Ab initio* Simulation Package (VASP) program.[15] To treat the van der Waals interaction among the molecules correctly, we added low-gradient (lg) pair-wise dispersion potential to the conventional Kohn–Sham DFT Hamiltonian.[16] *Ab initio* MD calculations were performed at 300 K using the canonical (NVT) ensemble for 30 ps using the VASP software.[15] The DFT calculations considered 8 $Li_4C_6O_6$ formula units. A plane-wave basis with a kinetic energy cut-off of 500 eV was used and reciprocal-space k-point meshes of $2 \times 2 \times 3$ were used to ensure that the total energies are converged within 5 meV per formula unit. The GCMC simulations were performed at 600 K with the Sorption module within the Cerius 2 software,[17] using 8 $Li_4C_6O_6$ formula units. The GCMC simulations used the DREIDING force-field parameters,[18] after optimization of the Li–O and Li–C parameters based on the quantum mechanical binding energies obtained from DFT calculation (GAUSSIAN 03 program[19] using Becke-Lee–Yang–Parr (B3LYP) hybrid exchange–correlation functional[20]).

Acknowledgements

This research was supported by (1) Energy Efficiency and Resources R&D program (20112020100070) under the Ministry of Knowledge Economy, Republic of Korea (2) Human Resources Development of the Korea Institute of Energy Technology Evaluation and Planning (KETEP) grant funded by the Korea government Ministry of Knowledge Economy (20114010203120) (3) WCU [World Class University programs through the National Research Foundation of Korea funded by the Ministry of Education, Science and Technology (R31-2008-000-10055-0)], and (4) the MSC/Caltech.

References

1 M. Armand and J.-M. Tarascon, *Nature*, 2008, **451**, 652.
2 H. Chen, M. Armand, G. Demailly, F. Dolhem, P. Poizot and J.-M. Tarascon, *ChemSusChem*, 2008, **1**, 348.
3 H. Chen, M. Armand, M. Courty, M. Jiang, C. P. Grey, F. Dolhem, J.-M. Tarascon and P. Poizot, *J. Am. Chem. Soc.*, 2009, **131**, 8984.
4 R. E. Dinnebier, H. Nuss and M. Jansen, *Acta Crystallogr., Sect. E: Struct. Rep. Online*, 2005, **61**, m2148.
5 K. Kang, D. Carlier, J. Reed, E. M. Arroyo, G. Ceder, L. Croguennec and C. Delmas, *Chem. Mater.*, 2003, **15**(23), 4503.
6 D. Carlier, L. Croguennec, G. Ceder, M. Menetrier, Y. Shao-Horn and C. Delmas, *Inorg. Chem.*, 2004, **43**(3), 914.
7 T. Matsumura, N. Sonoyama and R. Kanno, *Solid State Ionics*, 2003, **161**, 31.
8 K. Kang, C. H. Chen, B. J. Hwang and G. Ceder, *Chem. Mater.*, 2004, **16**, 2685.
9 K. Kang, D. Morgan and G. Ceder, *Phys. Rev. B*, 2009, **79**, 4.
10 D. Carlier, A. Van der Ven, C. Delmas and G. Ceder, *Chem. Mater.*, 2003, **15**, 2651.
11 M. S. Islam, D. J. Driscoll, C. A. J. Fisher and P. R. Slater, *Chem. Mater.*, 2005, **17**, 5085.
12 S. Grugeon, S. Laruelle, H. Chen, P. Poizot, P. Ribière, N. Recham, J.-M. Tarascon, M. Armand, *215th ECS Meeting*, San Francisco, CA, USA (2009).
13 Accelrys, *Material Studio Release Notes*, Release 5.5, Accelrys Software Inc.: San Diego, CA, 2006.
14 J. P. Perdew, K. Burke and M. Ernzerhof, *Phys. Rev. Lett.*, 1996, **77**, 3865.
15 G. Kresse and J. Furthmuller, *Comput. Mater. Sci.*, 1996, **6**, 15.
16 Y. Liu and W. A. Goddard, *J. Phys. Chem. Lett.*, 2010, **1**, 2550.
17 The Cerius2 Software, version 4.10, Accelrys Inc.: San Diego, CA.
18 S. L. Mayo, B. D. Olafson and W. A. Goddard, *J. Phys. Chem.*, 1990, **94**, 8897.
19 M. J. Frisch, G. W.T., H. B. Schlegel, G. E. Scuseria, M. A. Robb, J. R. Cheeseman, J. A. Montgomery, T. Vreven, K. N. Kudin, J. C. Burant, J. M. Millam, S. S. Iyengar, J. Tomasi, V. Barone, B. Mennucci, M. Cossi, G. Scalmani, N. Rega, G. A. Petersson, H. Nakatsuji, M. Hada, M. Ehara, K. Toyota, R. Fukuda, J. Hasegawa, M. Ishida, T. Nakajima, Y. Honda, O. Kitao, H. Nakai, M. Klene, X. Li, J. E. Knox, H. P. Hratchian, J. B. Cross, V. Bakken, C. Adamo, J. Jaramillo, R. Gomperts, R. E. Stratmann, O. Yazyev, A. J. Austin, R. Cammi, C. Pomelli, J. W. Ochterski, P. Y. Ayala, K. Morokuma, G. A. Voth, P. Salvador, J. J. Dannenberg, V. G. Zakrzewski, S. Dapprich, A. D. Daniels, M. C. Strain, O. Farkas, D. K. Malick, A. D. Rabuck, K. Raghavachari, J. B. Foresman, J. V. Ortiz, Q. Cui, A. G. Baboul, S. Clifford, J. Cioslowski, B. B. Stefanov, G. Liu, A. Liashenko, P. Piskorz, I. Komaromi, R. L. Martin, D. J. Fox, T. Keith, M. A. Al-Laham, C. Y. Peng, A. Nanayakkara, M. Challacombe, P. M. W. Gill, B. Johnson, W. Chen, M. W. Wong, C. Gonzalez, J. A. Pople; Gaussian, Inc.: *Gaussian 03, revision B. 03*, Pittsburgh, PA, 2003.
20 A. D. Becke, *J. Chem. Phys.*, 1993, **98**, 5648.